Geopersia ***8*** *(2), 2018, PP. 233-244* *DOI: 10.22059/geope.2018.245121.648358*

Enhanced chemical weathering and organic carbon burial as recovery factors for the OAE2 environmental conditions: a case study from Koppeh-Dagh Basin, NE Iran

Mohamad Hosein Mahmudy Gharaie*, Behnaz Kalanat
Department of Geology, Faculty of Science, Ferdowsi University of Mashhad, Mashhad, Iran
**Corresponding author, e-mail: mhmgharaie@um.ac.ir*
(*received: 04/11/2017 ; accepted: 05/05/2018*)

Abstract

A late Cenomanian-early Turonian interval (Hamam-ghaleh section) adjusted with the transition of Aitamir and Abderaz formations has been investigated in the east of Koppeh-Dagh Basin to examine geochemical anomalies and environmental perturbations related to the oceanic anoxic event 2 (OAE2). The study succession is composed of dark gray shale and glauconitic sandstone of Aitamir Formation, which is conformably overlain by cream marl and marly limestones of Abderaz Formation. The dark shale of the upper Aitamir Formation indicate higher organic matter concentrations especially in the two intervals at the end of *Rotalipora cushmani* biozone and at the middle part of *Whiteinella archaeocretacea* biozone. These intervals are characterized by higher detrital input (quartz and feldspar) and chemical alteration (high kaolinite/illite ratios), which suggest a warm-humid condition coeval with high productivity during the OAE2. The Aitamir Formation also shows higher total sulfur (TS) values associated with deposition of framboidal pyrite reflecting an oxygen deficiency, which provided favorable condition for reduction of sulfate. The warm and humid periods in the study section were followed by the cooler and drier intervals associated with decreased TOC values and chemical weathering. These cooling periods might be caused by falling of atmospheric CO_2 due to large amount of carbon burial in sediments and high silicate weathering. The $\delta^{13}C_{org}$ positive excursions of around 1‰ are other characteristics of these cooler-drier intervals, which were result of high burial of light carbon (^{12}C) in the organic matter and lower isotopic differentiation in low atmospheric pCO_2. At the top of study section, decrease of TOC and TS contents, low detrital input, decreased chemical weathering, and recovery of carbon isotope profile to the lower values indicate that the environmental conditions had returned to the normal oxygenated sea water after the OAE2.

Keywords*: Cenomanian/Turonian Boundary, Chemical Weathering, Koppeh-Dagh, OAE2, Organic Carbon Burial.*

Introduction

Global changes in climate, environment and oceanography leave the signatures in geochemical proxies of marine or terrestrial sedimentary records (Weissert *et al*., 2008). Characterization of depositional units and their correlation based on stratigraphic and geochemical variations initiated usage of the term "chemostratigraphy" that have been more frequent from the 1980s (Ramkumar, 2015).

The mid-cretaceous represents one of the most extensive geochemical anomalies in the Phanerozoic Eon, which has been largely studied based on chemostratigraphic analysis (Schlanger and Jenkyns, 1976; Arthur *et al*., 1985; Leckie *et al*., 2002; Jarvis *et al*., 2006; Voigt *et al*., 2006; Jenkyns, 2010; Jarvis *et al*., 2011, 2015 among others). During this episode dysoxia and anoxia referring to Oceanic Anoxic Events (OAEs; Schlanger and Jenkyns, 1976) occurred episodically across the marine basins (e.g., Schlanger and Jenkyns, 1976; Arthur *et al*., 1985; Takashima *et al*., 2009; Jenkyns, 2010). OAE2 at the Cenomanian/Turonian boundary (CTB; 93.6 Ma, Ogg *et al*., 2008) is one of the most prominent OAEs, which is characterized by the widespread organic rich sediments (Takashima *et al*., 2009) (Fig. 1-A), worldwide documented positive carbon isotope excursion in both carbonate ($\delta^{13}C_{carb}$) and organic matter ($\delta^{13}C_{org}$) (e.g., Scholle and Arthur, 1980; Arthur *et al*., 1988; Jarvis *et al*., 2006, 2011; Voigt *et al*., 2006; Jenkyns, 2010; Gavrilov *et al*., 2013), negative excursion in nitrogen isotope ratio ($\delta^{15}N$) (e.g., Junium and Arthur, 2007; Meyers *et al*., 2009; Baroni *et al*., 2015), and concentration of redox sensitive elements (e. g., Turgeon and Brumsak, 2006; Gavlilov *et al*., 2013).

The CTB in the Koppeh-Dagh Basin have spread out between Aitamir and Abderaz formations. This boundary have been studied for biostratigraphy and palaeoecology of planktonic and benthic foraminifera (Abdoshahi *et al*., 2010; Ghoorchaei *et al*., 2011; Kalanat *et al*., 2016, 2017b, 2018b) and palaeoenvironmental changes based on nitrogen isotope variations (Kalanat *et al*., 2017a). The main objective of our study is to evaluate the environmental perturbation across OAE2 on the Hamam-ghaleh section in the east of Koppeh-Dagh

Basin. Organic-carbon isotope ($\delta^{13}C_{org}$), total organic carbon (TOC) and total sulfur contents (TS) are combined with mineralogy data to provide an integrated chemostratigraphic correlation between the study section and other CTB successions in the koppeh-Dagh Basin and present a regional model to describe palaeoenvironmental condition in the basin.

Geological setting and study area

Koppeh-Dagh Basin

The formation and evolution of numerous continental blocks of Iran and surrounding area have been mainly controlled by the extensive orogenic activities during the opening and closure of Palaeotethys and Neotethys oceans (Bagheri and Stampfili, 2008). Palaeotethys was the ocean that separated Eurasian plate from the Gondwana (Muttoni *et al*., 2009). The northward subduction of this ocean generated the slab-pull forces on the Gondwana plate that led to detachment of Cimmerian blocks (including Iran, central Afghanistan, Karakoram, Pamir, etc.) and opening of Neotethys ocean (Bagheri and Stampfili, 2008). Continuing subduction of Palaeotethys ocean and northward drifting of the Cimmerian blocks finally led to collision of Iranian plate and Turan plate (Eurasia) around the middle-late Triassic resulting in the early Cimmerian orogeny (Bagheri and Stampfili, 2008; Robert *et al*., 2014). After this collision the deposition of Koppeh-Dagh Basin started on the southern margin of Eurasian plate in a narrow shelf and continental slope environments. This basin covers an area of over 500 km^2 in the northeast of Iran (Fig. 1B) with more than 7000 m-thick sediments including carbonate, siliciclastic and evaporate from Jurassic to Neogene (Afshar-Harb, 1979; Robert *et al*., 2014).

The Aitamir (Albian-Cenomanian) and Abderaz (Turonian to early Campanian) are two widespread upper Cretaceous formations in the Koppeh-Dagh Basin (Fig. 2). There is a conformable transition between the two formations based on planktonic foraminiferal studies and lithostratigraphic data in the east of Koppeh-Dagh Basin (Mokhtari *et al*., 1999; Abdoshahi *et al*., 2010; Goorchaei *et al*., 2011; Kalanat *et al*., 2016).

Hamam-ghaleh section

The Hamam-ghaleh section is located in the east of Koppeh-Dagh Basin, 7km south to Kalate-Nader City, near the Hamam-ghaleh village (Fig. 1B and 1C). The studied succession is composed of 26 m-thick dark gray shale and glauconitic silty sandstone of Aitamir Formation with low abundance of benthic and planktonic foraminifera and high concentration of framboidal pyrite. It is conformably overlain by 22 m-thick cream marl and marly limestones of Abderaz Formation, which are characterized by high diversity of foraminifera and lack of framboidal pyrite.

The section has been previously studied based on planktonic foraminifera (Goorchaei *et al*., 2011), and three biozones, namely, *Roralipora cushmani, Whiteinella archaeocretacea* and *Helvetoglobotruncana helvetica* (Premoli-Silva and Verga, 2004) have been reported, spanning from late Cenomanian to early Turonian. The CTB lies in the *W. archaeocretacea* biozone, but the exact horizon of the boundary cannot be specified by planktonic foraminifera.

Materials and Methods

36 powdered and de-carbonated samples (8 shale, 4 sandstone, 25 marl and marly limestone) were analyzed for TOC, TS and $\delta^{13}C_{org}$ at Department of Earth and Planetary Science, University of Tokyo (Table 1). For C and S analysis, ca. 20 mg of each samples were measured using a Thermo Finnigan Flash EA 1112 series CNS analyzer using a retention time of 720 s. The analytical error was less than 0.2 wt% for TOC, and <0.1 wt% for TS, using sulfamethazine standard.

Ca. 1.5 mg of samples were analyzed for $\delta^{13}C_{org}$ by a combination system of Thermo Finnigan Flash EA 1112 series analyzers, CONFLO III, and Delta Plus mass spectrometer. The values were expressed in per mil (‰) relative to the Vienna Pee Dee Belemnite (VPDB) with the analytical error of <0.1% using standard IAEA-C6 sucrose.

Bulk rock mineralogy was determined using an Ultima IV X-Ray Diffractometer at Department of Earth and Planetary Science, University of Tokyo.

Results

Total organic carbon and total sulfur (TOC and TS)

TOC values in the Hamam-ghaleh section range between 0.083% and 0.83%. Two organic-rich intervals occur at the end of *R. cushmani* and the middle part of *W.archaeocretacea* biozones. Generally, the Aitamir Formation shows relatively-higher organic matter contents with the average value of 0.5%, whereas TOC values in the Abderaz Formation are low and oscillate around a mean of 0.13%. The Aitamir Formation also shows mean

sulfur content of 0.07% and two outliners of 0.32% and 0.24% occur at samples HM5 and HM10 respectively, while the TS contents in the most samples of the Abderaz Formation are almost 0% (Table 1, Fig. 3).

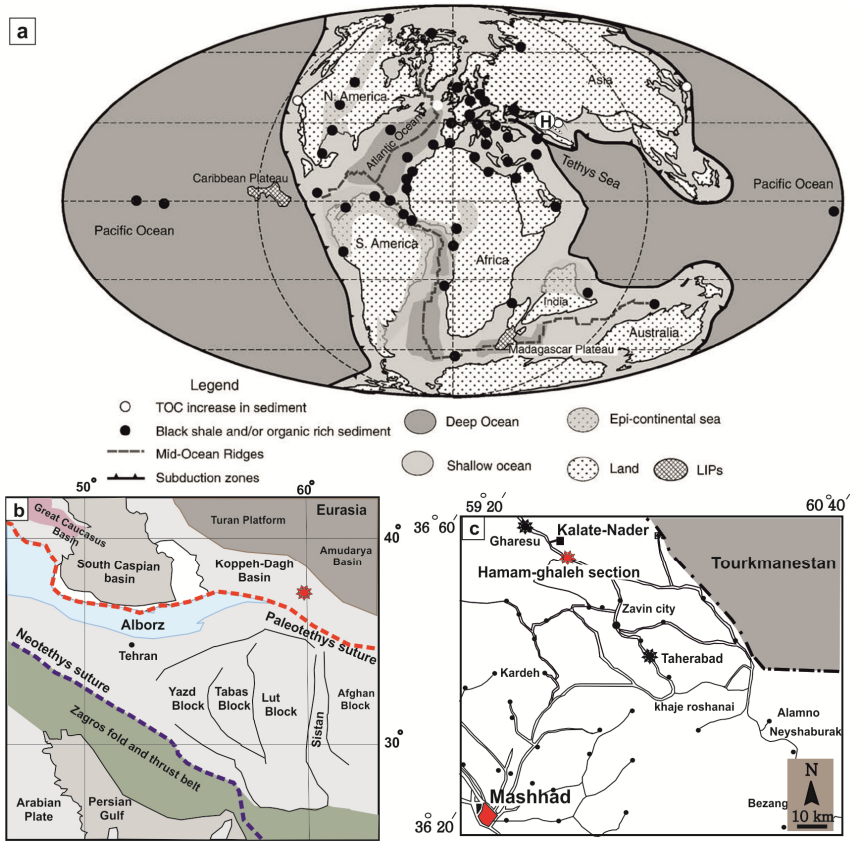

Figure 1. a- Distribution of black shales and organic-rich sediments around the Cenomanian/Turonian boundary (Modified after Takashima *et al*., 2009). The position of Hamam-ghaleh section is specified by H. b- Map of Iran and surrounding areas. Neotethys and Paleotethys sutures zones, Koppeh-Dagh Basin and study area are indicated (modified after Angiolini *et al*., 2007). c- Locality map of Hamam-ghaleh section in 7 km south of Kalate-Nader city.

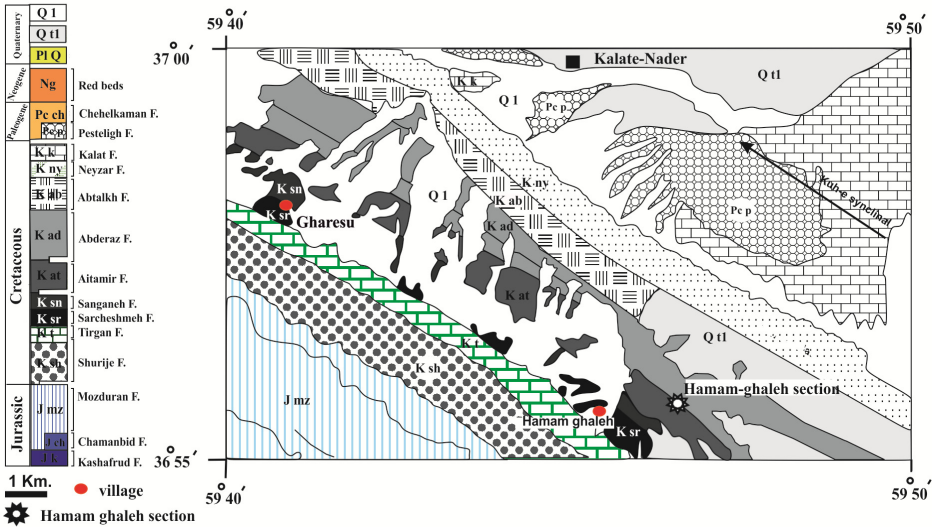

Figure 2. A part of 1/100000 geological map of Kalate-Nader in the east of Koppeh-Dagh Basin (Nabavieh, 1998). The location of Hamam-ghaleh section laying in the Aitamir-Abderaz formations transition is indicated by star.

Table 1. TOC, TS and $\delta^{13}C_{org}$ of the late Cenomanian-early Turonian sequence in Hamam-ghaleh section, Koppeh-Dagh Basin.

Sample No.	Height (m)	TOC (%)	TS (%)	$\delta^{13}C_{org}$ (‰)	Sample No.	Height (m)	TOC (%)	TS (%)	$\delta^{13}C_{org}$ (‰)
HM 0	0	0.45	0	-	HM18	30	0.17	0	-26.30
HM1	1.5	0.73	$7.6*10^{-3}$	-26.68	HM 19	30.5	0.17	0	-26.67
HM2	3	0.83	0.07	-27.02	HM20	31	0.19	0	-26.63
HM3	4.5	0.35	0.04	-27.13	HM21	31.5	0.11	0	-26.60
HM4	5.5	0.36	0.02	-26.52	HM22	32.5	-	0	-
HM5	8.5	0.40	0.32	-	HM23	33.5	0.14	0	-
HM6	11	0.34	0.07	-26.78	HM24	34.5	0.10	0	-
HM7	13.5	0.54	0	-27.33	HM25	35.5	0.12	0	-
HM8	17	0.43	0.05	-27.14	HM26	36.5	0.12	0	-26.39
HM9	19	0.53	0.03	-27.35	HM27	37.5	0.20	0	-26.25
HM10	21	0.55	0.24	-27.20	HM28	38.5	0.13	$5.7*10^{-3}$	-26.85
HM10b	23	0.60	0.03	-27.28	HM29	39.5	0.10	0	-26.58
HM11	24.5	0.40	0	-27.19	HM30	40.5	0.11	0	-26.70
HM12	26.5	0.15	0	-27.19	HM31	41.5	0.13	0	-27.27
HM13	27	0.08	0	-26.21	HM32	42.5	0.08	0.02	-26.66
HM14	27.5	0.12	0	-26.66	HM33	43.5	0.15	0	-27.07
HM15	28	0.10	0	-26.48	HM34	44	0.08	0	-26.02
HM16	28.5	0.13	0	-26.71	HM35	45.5	0.15	0	-26.83
HM17	29.5	-	-	-	HM36	48	0.15	0	-27.09

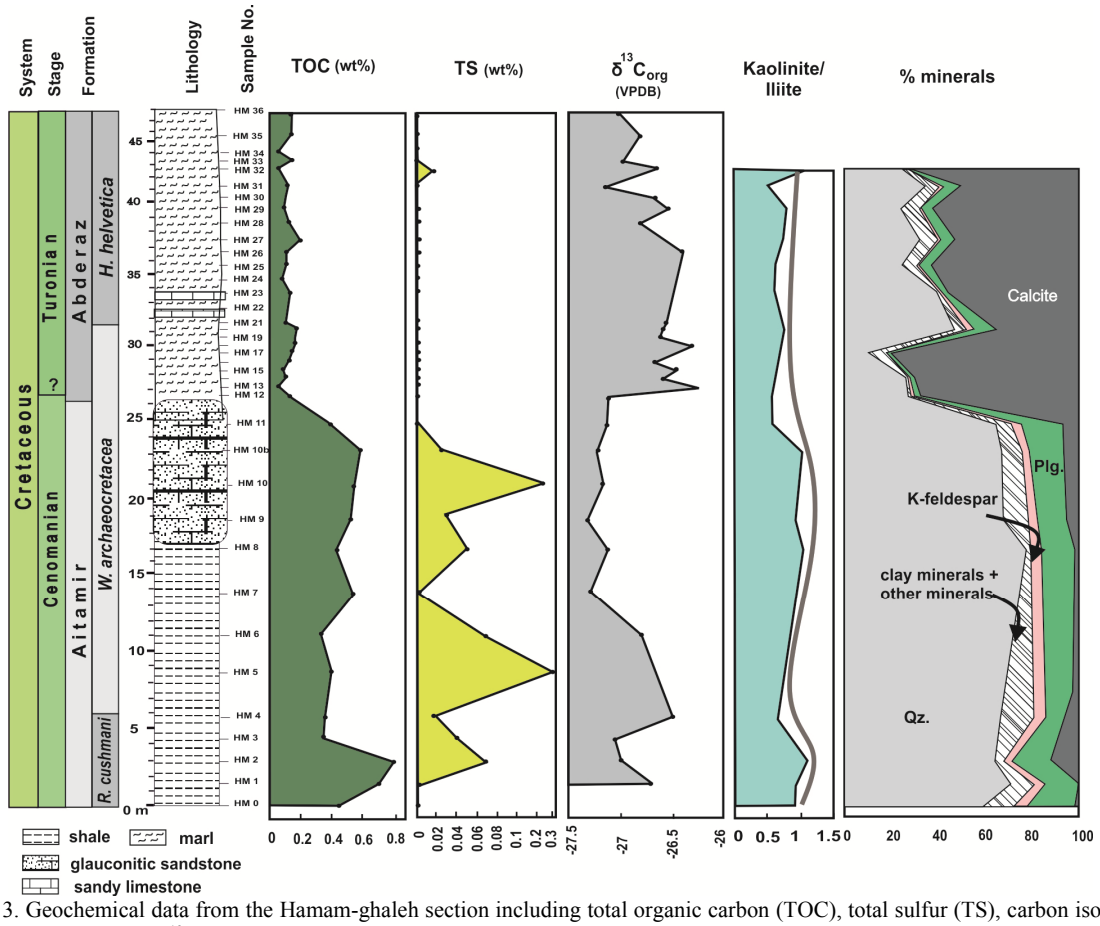

Figure 3. Geochemical data from the Hamam-ghaleh section including total organic carbon (TOC), total sulfur (TS), carbon isotope in organic matter fraction ($\delta^{13}C_{org}$), kaolinite/illite ratio as chemical weathering proxy and bulk rock mineralogy.

Mineralogy

The bulk rock compositions in the lower part of the studied section (Aitamir Formation) consist mostly of quartz (61-78%) and feldspar (plagioclase + Kfeldespar, 15-24%). Minor components include calcite (0.7- 11%) and clay minerals (3-10%). A marked increase in calcite (50-80%) and decrease in detrital components (quartz and feldspar) have been observed in the upper part of the section (Abderaz Formation). This change reflects the lithological transition from shale and sandstone of Aitamir Formation to marlstone and marly limestone of Abderaz Formation (Fig. 3).

Carbon isotopes

The $\delta^{13}C_{org}$ values in the studied section varies between -25.85‰ and -27.35‰. The values show a positive excursion to -26.52‰ at the end of *R. cushmani* biozone (HM4), and then decrease down to -27.35‰ at the middle part of *W. archaeocretacea* biozone (HM9), followed by an increase to -26.21‰ at sample HM13. After that the $\delta^{13}C_{org}$ curve shows a negative trend until the top of the studied succession (Tab.1, Fig.3).

Discussion

TOC and TS in the Hamam-ghaleh section

Generally organic matter burial is mainly controlled by primary productivity and preservation. Organic carbon flux to the sea-floor is depended on such variable factors as enhanced runoff, intensified upwelling and fertilization of oceanic water by volcanically derived metals like Fe. On the other hand, preservation proposes reduced decomposition of organic matter as a result of decreased bottom water oxygen levels and/or high sedimentation rate (Demaison and Moore, 1980; Canfield, 1994; Meyers, 1997; Meyers *et al*., 2006). In reality, both productivity and preservation have a crucial role in forming black shale deposits, but the plankton productivity is commonly the most important (Pedersen and Calvert, 1990, Jenkyns *et al*., 2002).

OAE2 is characterized by widespread deposition of black shale in the deep water, upwelling zones (e.g. Voigt *et al*., 2006; Junium & Arthur, 2007; Mort *et al*., 2008) and restricted areas (e.g. Leckie *et al*., 1998; Elderbak *et al*., 2014), however some shallow water and coastal areas are black shale-free (Keller *et al*., 2008; Gertsch *et al*., 2010). CTB interval is also characterized by high TS contents (Wortmann *et al*., 1999; Brumsack, 2006; Okano *et al*., 2007; Hetzel *et al*., 2009), because the oxygen deficiency increases sulfate reduction and sulfide formation like pyrite in the sediments (Dean *et al*., 2013).

The Hamam-ghaleh section contains two TOC-enriched intervals (Fig. 3). The lower and larger one (up to 0.8 %) is at the base of section (end of *R. cushmani* biozone) and the second one covers the upper part of Aitamir Formation at the middle part of *W. archaeocretacea* biozone. The TOC-enriched intervals accompanied by higher TS contents and presence of framboidal pyrite, implying the effect of OAE2 and expansion of oxygen deficiency in the upper Aitamir Formation, whereas the total sulfur in the following interval (Abderaz Formation) decline to zero percent (except for the sample HM32) (Fig 3). Beside the expansion of oxygen minimum zone, higher TOC contents in the Aitamir Formation could be result of higher accumulation rate and/or delivery of the terrestrial organic matter into the basin.

Comparison of TOC profile in the Hamam-ghaleh section with two other sections in the east of Koppeh-Dagh basin (Gharesu and Taherabad sections; Fig. 4) reveals that black shale is not deposited in this part of basin. The TOC contents and position of organic-enriched intervals in the Aitamir Formation are almost similar (Kalanat *et al*., 2017b; Kalanat *et al*., 2018b).

Mineralogy and palaeo-climate condition

Kaolinite and illite are two major clay mineral components in the Hamam-ghaleh section. Kaolinite as a product of chemical weathering forms under humid condition (Parrish, 1998; Schnyder *et al*., 2005; Gertsch *et al*., 2010), whereas illite is an indicative of moderate climate and low intensity of chemical alteration (Singer, 1984; Oliveira *et al*., 2002). The concept of kaolinite/illite ratio, which is called “clay mineral index” can be used as palaeo-climate proxy (Robert and Kennet, 1994, 1997; Mahmudy Gharaie *et al*., 2004) in chemostratigraphy.

Kaolinite/illite ratio in the study succession indicates relatively higher values in the Aitamir Formation especially in the two organic matter-enriched intervals. Higher clay mineral index accompanied with large values of detrital minerals in the Aitamir Formation reflect a warm and humid condition with higher chemical weathering and enhanced runoff into the basin in the late Cenomanian. A dramatic decrease in detrital input (deposition of carbonate dominant sediments) from Aitamir up to the Abderaz formations, and

relatively lower kaolinite/illite ratios can be interpreted as a cooler and drier climate with reduced chemical weathering and runoff into the basin.

Carbon stratigraphy of the CTB

Carbon isotopes are not so sensitive to diagenetic alterations, therefore potentially provide excellent information about changes in global carbon cycle, particularly variation in the burial rate of organic matter. It also can be used as palaeoenvironmental proxy for volcanogenic CO_2 supply, weathering rate, changes in ocean circulation and release of methane from the clathrate in the sea floor (Pearce *et al*., 2009).

The CTB interval is characterized by a major global positive excursion of $\delta^{13}C$ that occurs in marine carbonate, and both marine and terrestrial organic matter (Arthur *et al*., 1988; Jarvis *et al*., 2006, 2011; Caron *et al*., 2006). This is mainly attributed to the widespread removal of isotopically light carbon (^{12}C) from the carbon cycle, due to increased biological production and/or increased preservation of organic matter (Schlanger and Jenkyns, 1976; Scholle and Arthur, 1980; Arthur *et al.,* 1985, 1988). The $\delta^{13}C_{org}$ values are also partially controlled by the isotope fractionation associated with photosynthesis (ε_p), whereas organic matter provided in lower atmospheric pCO_2 is relatively ^{12}C-depleted (van Bentum *et al*., 2012).

In the CTB, superimposed on the long-term positive carbon excursion, some major features in $\delta^{13}C$ pattern can be identified. Such general pattern in $\delta^{13}C$ data has been first reported by Pratt and Threlkeld (1984) as an initial enrichment ("A"), a brief recovery ("B"), and a sustained plateau ("C"), which subsequently found in a globally correlation (e.g., Jarvis *et al*., 2006). The alternative view is that $\delta^{13}C$ profile across the CTB includes three peaks, where the upper two peaks appear as two small projections on a broad peak (e. g., Caron *et al*., 2006; Takashima *et al*., 2009; Pearce *et al*., 2009; Jarvis *et al*., 2011).

During the past decades, the carbon stratigraphic correlation has been examined using biostratigraphic datum levels (e.g., Bengtson, 1996; Caron, 2006; Jervis, 2011).

These studies indicates that the last $\delta^{13}C$ peak occurs around the CTB, but minor differences are attributed to preservation factors associated with facies changes and/or difficulties in precisely placing the datum levels (Caron *et al*., 2006).

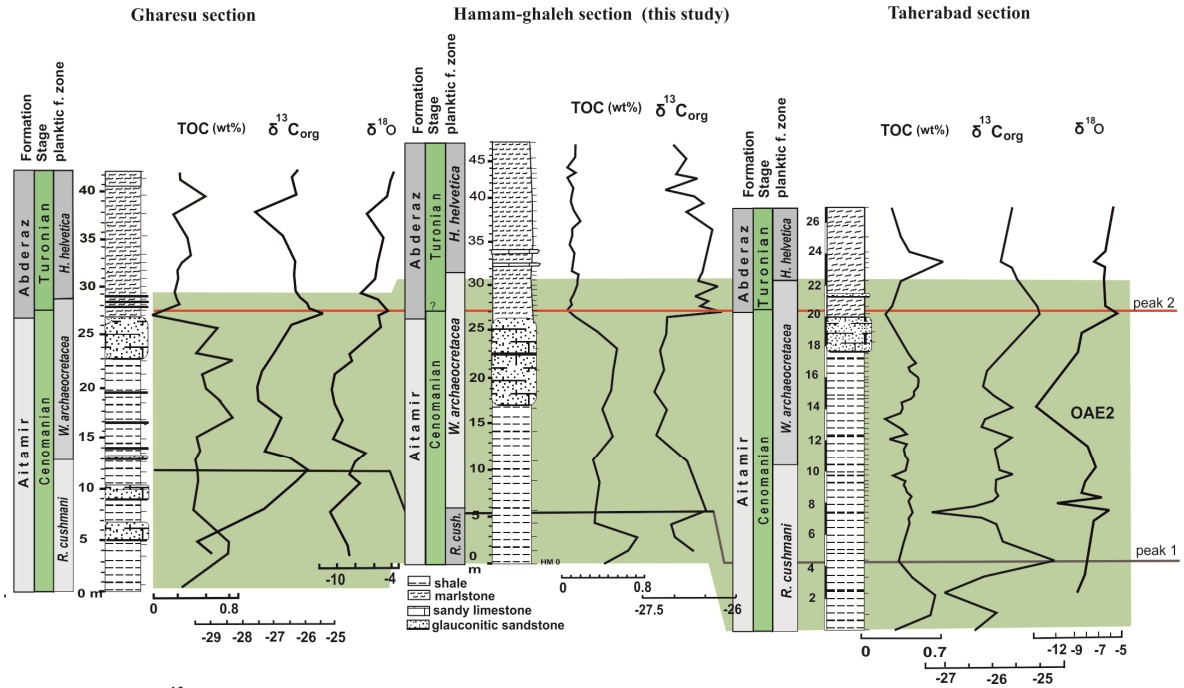

Figure 4. TOC and $\delta^{13}C_{org}$ in the Hamam-ghaleh, Gharesu and Taherabad sections. Horizontal lines show correlation of major carbon isotope peaks. The geochemical data for Gharesu section are from Kalanat *et al*. (2018b) and for Taherabad section are based on Kalanat *et al*. (2018a). The green band indicates interval of higher TOC bearing deposits and positive $\delta^{13}C$ excursion defining Oceanic Anoxic Event 2.

At the Hamam-ghaleh section the excursion begins at the top of *R. cushmani* biozone (sample HM4), followed by a brief recovery around the middle part of *W. archaeocretacea* biozone (HM7-HM12), and a longer positive excursion at the top of this biozone (HM13-HM18). The excursion ends at the upper part of section in the *H. helvetica* biozone (Fig 3). The second and the last large peak in the study succession occurs after sandstone unit and is considering as position of CTB.

Comparison of $\delta^{13}C_{org}$ values to other sections

the CTB $\delta^{13}C_{org}$ excursion shows the amplitude as much as 4‰ in many localities such as Atlantic region (Arthur *et al*., 1988; Kuypers *et al*., 2002; Sinninghe Damsté *et al*., 2008) Boreal Sea (Tsikos *et al*., 2004) and Tethys Ocean (Jarvis *et al*., 2011).

The $\delta^{13}C_{org}$ excursion value in the study area is about 1‰, whereas the other CTB Koppeh-Dagh sections in the Gharesu and Taherabad (Kalanat *et al*., 2018a, b), also reveal greater positive shifts about 2.5‰ and 2‰, respectively (Fig. 4). These differences may be caused by varying sedimentation rate of terrestrial organic matter in the shallow environments, which were transported from continent into the basin.

Apart from the larger $\delta^{13}C_{org}$ positive shifts in the Gharesu and Taherabad sections than the study succession, the sharp excursion and stratigraphic position of major shifts in the upper part of *R. cushmani* and *W. archaeocretacea* biozones are comparable. The recovery phase after the first excursion seems too negative in these sections (even more negative than post OAE2 interval) in compare to other sections in the world (e.g. Caron, 2006; Jervis, 2011), which can be explained by enhanced fluvial delivery of isotopically light inorganic carbon recycled from soil organic matter. Only some of these material would need to be oxidized and make the isotopic composition of photic zone carbon pool lighter (Meyers *et al*., 2006). This hypothesis can be confirmed in the study area by correspondence of the intervals characterizing by enhanced run off and low $\delta^{13}C_{org}$ values (Fig. 6).

Palaeoenvironmental model

Figure 5 is a simple diagram representing the factors controlling palaeoenvironmental perturbation and climate changes during the OAE2. It proposes that the event was triggered by emplacement of Caribbean Plateau providing CO_2 out-gassing and consequence greenhouse condition (Arthur *et al*., 1985; Larson, 1991; Leckie *et al*., 2002; Snow and Duncan, 2005; Seton *et al*., 2009), acceleration of hydrological cycle and enhanced chemical weathering (Fletcher *et al*., 2008; Barclay *et al*., 2010; Pogge von Strandmann *et al*., 2013), high nutrient input, biological productivity and carbon flux to the sea floor (Jones and Jenkyns, 2001), which finally led to fostering the organic matter-enriched sediments.

The high burial rate of carbon in the organic-enriched deposits of CTB was a powerful factor to draw down atmospheric CO_2 and cause the consequent cooling of the global climate (Arthur *et al*., 1988; Freeman and Hayes, 1992; Kuypers *et al*., 1999). Weathering of silicate minerals also can remove CO_2 from the atmosphere (For example, $2CO_2 + 4H_2O + CaA1_2Si_2O_8 \rightarrow Ca^{++} + 2Al(OH)_3 + 2SiO_2^{aq} + 2HCO_3^-$; Brady, 1991) and reduce the temperature (Pogge von Strandmann *et al*., 2013). Therefore, it can be concluded that the warm and humid intervals with high burial of organic carbon and intensified chemical weathering during the CTB could subsequently turn into cold and drier intervals (Fig. 5).

This process can be followed in our study succession (Fig. 6). Two high TOC intervals coincide with warm-humid conditions, high chemical weathering and high detrital input. We propose that surface runoff provide low-density fresh water cap, which led to water column stratification. These conditions coeval with high productivity due to high nutrient input and influx of organic matter to the sea floor resulted in low oxygen condition, better preservation of organic matter and favorite environment for deposition of framboidal pyrite (Fig. 6a). The subsequent intervals are characterized by lower TOC contents, decreased chemical weathering and increased $\delta^{13}C_{org}$ values, which caused by cooler and drier condition (Fig. 6b). The $\delta^{13}C_{org}$ values returned to lower values in upper part of the section indicating a normal marine conditions and generally well-oxygenated seafloor after the OAE2. This model refers to the worldwide conditions for the basins during the CTB, which were not influenced by upwelling systems (e.g. Cuba section in the Western Interior Seaway, Elderbak *et al*., 2014) and can be well defined for the Gharesu and Taherabad sections in the east of Koppeh-Dagh Basin.

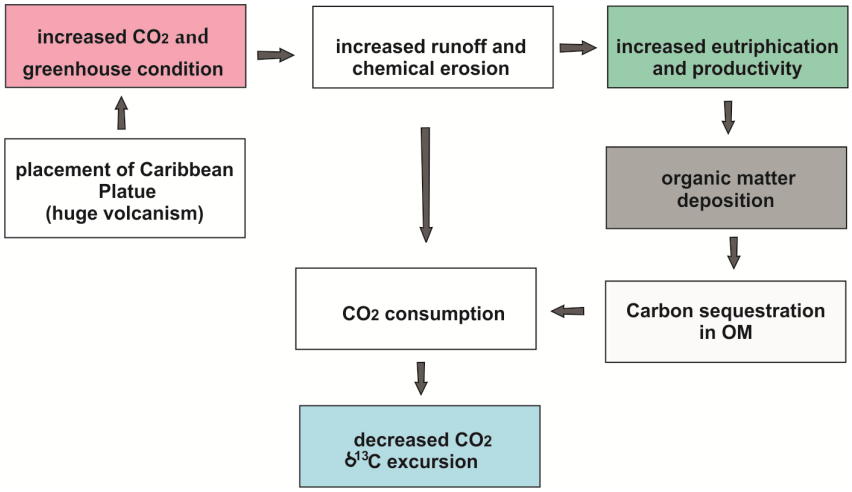

Figure 5. Factors controlling palaeoenvironmental perturbation and climate changes during the OAE2.

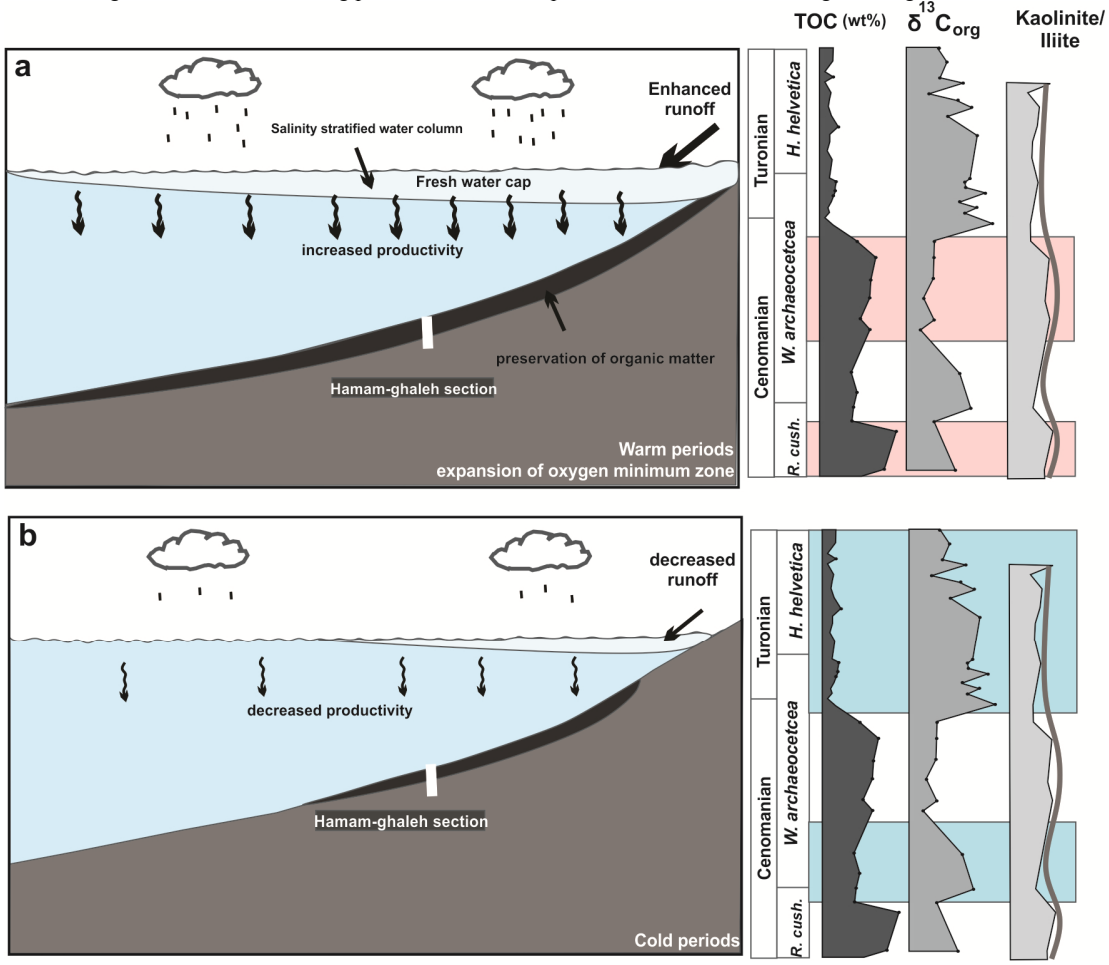

Figure 6. Palaeoenvironmental changes across late Cenomanian-early Turonian of Hamam-ghaleh section. A model proposed based on TOC content, chemical weathering index and $\delta^{13}C_{org}$.

In these sections the intervals of warm-humid conditions are coeval with lower $\delta^{18}O$ values and higher TOC. Inversely, the cooler and drier intervals are characterized by higher $\delta^{18}O$ values and lower TOC contents, which can confirm this model (Fig. 4).

Conclusion

Global warming, accelerated hydrological cycle and

enhanced marine primary productivity all have been suggested as having contribution to the occurrence of widespread ocean anoxia during the OAE2, but recognizing these factors on a regional scale has remained problematic. In an attempt to separate these forcing factors, we generated geochemical record in a late Cenomanian-early Turonian succession in the east of Koppeh-Dagh Basin laying in the Aitamir-Abderaz formations transition.

However TOC<1% in the study section indicates that the extensive anoxia have not been occurred in the region but higher TOC and TS, increased detrital input and kaolinite/illite ratios (as chemical weathering proxy) in two intervals of the Aitamir Formation indicate that greenhouse condition during OAE2 accelerated chemical weathering and runoff in to the basin. This condition in turn would have led to enhanced nutrient supply and productivity in the basin and either water column stratification.

Increased global burial of organic matter and CO_2 consumption due to silicate weathering resulted in falling atmospheric CO_2 and provide a relatively cooler and drier conditions, which are characterized by lower TOC values, decreased detrital input and chemical weathering. These cold intervals were also demonstrated by $\delta^{13}C_{org}$ excursion because organisms preferentially take up light carbon^{12}C to produce organic matter. Also, it has been proposed that the rate of isotopic fractionation during carbon fixation by phytoplankton decreases at lower *p*CO2 values, which led to positive $\delta^{13}C_{org}$ excursion.

The acquiesced data from Hamam-ghaleh section indicate that upper part of the Aitamir Forrmation was deposited under the OAE2 impressions, but toward the Abderaz Formation the environment returned into the normal marine condition, which provided favorite situation for carbonate production and deposition of marl and limestone of the Abderaz Formation.

Acknowledgements

This study was conducted as the research project #2/43229 supported by Ferdowsi University of Mashhad. The authors would like to express their sincere thanks to Professor Ryo Matsumoto for arrangement of the geochemical analysis in the University of Tokyo, Japan. Thanks are also extended to Dr. Mohamad Vahidinia (F.U.M.) for field support and introducing the section in Hamam-ghaleh area in NE Mashhad and to Mrs. Leili Fateh Bahary for her kindly collaboration in field and laboratory works.

References

Abdoshahi, M., Vahidinia, M., Ashuri, A., Rahimi, B., 2010. Microbiostratigraphy of Cenomanian/Turonian boundary in the Shurab section, east of Kopet-Dagh basin. Sedimentary Facies, 1: 61-70 (In Persian).

Afshar-Harb, A., 1979. The stratigraphy, tectonics and petroleum peology of the Kopet Dagh region, Northern Iran. Ph.D. thesis, University of London. 316 pp.

Angiolini, L., Gaetani, M., Muttoni, G., Stephanson, M.H., Zanchi, A., 2007. Tethyan oceanic currents and climate gradients 300 m.y. ago. Geology, 35: 1071-1074.

Arthur, M.A., Dean, W.E., Pratt, L.M., 1988. Geochemical and climatic effects of increased marine organic carbon burial at the Cenomanian/Turonian boundary. Nature, 335: 714-717.

Arthur, M.A., Dean, W.E., Schlanger, S.O., 1985. Variations in the global carbon cycle during the Cretaceous related to climate, volcanism and changes in atmospheric CO_2, in The Carbon Cycle and Atmospheric CO_2. In: Sundquist, E.T., Broecker, W.S. (Eds.), Natural Variations Archean to Present. Geophysical Monograph Series, pp. 504-529.

Bagheri, S., Stampfli, G.M., 2008. The Anarak, Jandaq and Posht-e-Badam metamorphic complexes in central Iran: new geological data, relationships and tectonic implications. Tectonophysics, 451: 123–155.

Barclay, R.S., Mc Elwain, J.C., Sageman, B.B., 2010. Carbon sequestration activated by a volcanic CO_2 pulse during Ocean Anoxic Event 2. Nature Geoscience, 3: 205-208.

Baroni, I.R., van Helmond, N.A.G.M., Tsandev, I., Middelburg, J.J., Slomp, C.P., 2015. The nitrogen isotope composition of sediments from the proto-North Atlantic during Oceanic Anoxic Event 2. Paleoceanography, 30: 923-937.

Bengtson, P., 1996. The Turonian stage and substage boundaries. In: Rawson, P.F., Dhont, A.V., Hancock, J.M., Kennedy, W.J. (Eds.), Proceedings« Second International Symposium on Cretaceous Stage Boundaries » Brussels 1995. Bulletin de l'Institut Royal des Sciences Naturelles de Bel-gique, pp. 69-79.

Brady, P.V., 1991. The effect of silicate weathering on global temperature and atmospheric CO_2. Journal of Geophysical Research, 96: 101-106.

Brumsack, H.J., 2006. The trace metal content of recent organic carbon-rich sediments: Implications for Cretaceous black

shale formation. Palaeogeography, Palaeoclimatology, Palaeoecology, 232: 344-361.
Canfield, D.E., 1994. Factors influencing organic carbon preservation in marine sediments. Chemical Geology, 114: 315-329.
Caron, M., Dall'Agnolo, S., Accarie, H., Barrera, E., Kauffman, E.G., Amedro, F., Robaszynski, F., 2006. High-resolution stratigraphy of the Cenomanian/Turonian boundary interval at Pueblo (USA) and wadi Bahloul (Tunisia): stable isotope and bio-events correlation. Geobios, 39: 171-200.
Dean, W.E., Arthur, M.A., Claypool, G.E., 1986. Depletion of ^{13}C in Cretaceous marine organic matter: source, diagenetic, or environmental signal?. Marine Geology, 70: 119-157.
Dean, W.E., Kauffman, E.G., Arthur, M.A., 2013. Accumulation of organic carbon-rich strata along the western margin and in the center of the North American western interior seaway during the Cenomanian-Turonian Transgression. In: Titus, A.L., Loewen, M.A. (Eds.), At the top of the Grand Staircase: The Late Cretaceous of Southern Utah. Indiana University Press, pp. 42-56.
Demaison, G.T., Moore, G.T., 1980. Anoxic environments and oil source bed genesis. Organic Geochemistry, 2: 9-31.
Elderbak, K., Leckie, R.M., Tibert, N.E., 2014. Paleoenvironmental and paleoceanographic changes across the Cenomanian/Turonian boundary Event (Oceanic Anoxic Event 2) as indicated by foraminiferal assemblages from the eastern margin of the Cretaceous Western Interior Seaway. Palaeogeography, Palaeoclimatology, Palaeoecology, 413: 29-48.
Fletcher, B.J., Brentnall, S.J., Anderson, C.W., Berner, R.A., Beerling, D.J., 2008. Atmospheric carbon dioxide linked with Mesozoic and Early Cenozoic climate change. Nature Geoscience, 1: 43- 48.
Freeman, K.H., Hayes, J.M., 1992. Fractionation of carbon isotopes by phytoplankton and estimates of ancient CO2 levels. Global Biogeochemical Cycles, 7(2): 185-198.
Gavrilov, Y.O., Shcherbinina, E.A., Golovanova, O.V., Pokrovskii, B.G., 2013. The Late Cenomanian Paleoecological Event (OAE 2) in the Eastern Caucasus Basin of Northern Peri-Tethys. Lithology and Mineral Resources, 48: 457-488.
Gertsch, B., Adatte, T., Keller, G., Tantawy, A.M., Berner, Z., Mort, H., Fleitmann, D., 2010. Middle and late Cenomanian ocanic anoxic event in shallow and deepr shelf environment of western Morocco. Sedimentology, 10: 1-33.
Ghoorchaei Sh., Vahidinia, M., Ghasemi-Nejad, E., Mahmudy-Gharaie, M.H., 2011. Microbiostratigraphy of Cenomanian/Turonian boundary in the Hamam-ghaleh section, east of Kopet-Dagh basin. Journal of Geology of Iran, 19: 31-44. (in Farsi).
Hetzel, A., Bottcher, M.E., Wortmann, U.G., Brumsack, H.J., 2009. Paleo-redox conditions during OAE2 reflected in Demerara Rise sediment geochemistry (ODP Leg 207). Palaeogeography, Palaeoclimatology, Palaeoecology, 273: 302-328.
Jarvis, I., Gale, A.S., Jenkyns, H.C., Pearce, M.A., 2006. Secular variation in Late Cretaceous carbon isotopes and sea-level change: Evidence from a new $\delta^{13}C$ carbonate reference curve for the Cenomanian-Campanian (99.6–70 .6 Ma). Geological Magazine, 143: 561-608.
Jarvis, I., Lignum, J.S., Gröcke, D.R., Jenkyns, H.C., Pearce, M.A., 2011. Black shale deposition, atmospheric CO_2 drawdown and cooling during the Cenomanian-Turonian Oceanic Anoxic Event. Paleoceanography, 26: PA3201.
Jarvis, I., Trubucho-Alexandre, J., Gröcke, D.R., Ulicny, D., Laurin, J., 2015. Intercontinental correlation of organic carbon and carbonate stable isotope records: evidence of climate and sea-level change during the Turonian (Cretaceous). The Depositional Record, 1(2): 53-90.
Jenkyns, H.C., 2010. Geochemistry of oceanic anoxic events, Geochemictary, Geophysics, Geosystems, 11: Q03004.
Jenkyns, H.C., Jones, C.E., Gröcke, D.R., Hesselbo, S.P., Parkinson, D.N., 2002. Chemostratigraphy of the Jurassic System: Applications, limitations and implications for palaeoceanography. Journal of Geology Society, 159: 351-378.
Jones, C.E., Jenkins, H.C., 2001. Seawater strontium isotopes, oceanic anoxic events, and sea floor hydro-thermal activity in the Jurassic and cretaceous. American Journal of Science, 301: 112-149.
Junium, C.K., Arthur, M.A., 2007. Nitrogen cycling during the Cretaceous, Cenomanian-Turonian Oceanic Anoxic Event II. Geochemistary, Geophysic, Geosystems, 8: 1-18.
Kalanat, B., Mahmudy Gharaie, M.H., Vahidinia, M., Matsumoto, R., 2018a. Short-term eustatic sea-level changes during the Cenomanian–Turonian Supergreenhouse interval in the Kopet-Dagh Basin, NE Tethyan realm. Journal of Iberian Geology, 44(2): 177-191.
Kalanat, B., Mahmudy Gharaie, M.H., Vahidinia, M., Vaziri-Moghaddam, H., Kano, A., 2017a, Nitrogen isotope variations and environmental perturbations during Cenomanian-Turonian transition in the NE Tethyan realm, Kopet-Dagh basin. Geopersia, 7(1): 1-9.
Kalanat, B., Mahmudy Gharaie, M.H., Vahidinia, M., Vaziri-Moghaddam, H., Kano, A., Kumon, F., 2018b. Paleoenvironmental perturbation across the Cenomanian/Turonian boundary of the Kopet-Dagh Basin (NE Iran), inferred from geochemical anomalies and benthic foraminiferal assemblages, Cretaceous Research, 86: 261-275.
Kalanat, B., Vahidinia, M., Vaziri-Moghaddam, H., Mahmudy Gharaie, M.H., 2016. Planktonic foraminiferal turnover

across the Cenomanian/Turonian boundary (OAE2) in northeast of Tethys realm, Kopet-Dagh basin. Geologica Carpathica, 67: 451-462.

Kalanat, B., Vahidinia, M., Vaziri-Moghaddam, H., Mahmudy Gharaie, M.H., Kumon, F., 2017b, Benthic foraminiferal response to environmental changes across Cenomanian/Turonian boundary (OAE2) in the northeastern Tethys, Kopet-Dagh basin. Journal of African Earth Science, 134: 33-47.

Keller, G., Tantawy, A.A., Berner, Z., Adatte, T., Chellai, E.H., Stueben, D., 2008. Oceanic events and biotic effects of the Cenomanian–Turonian anoxic event, Tarfaya Basin, Morocco. Cretaceous Research, 29: 976-994.

Kuypers, M.M.M., Pancost, R.D., Nijenhuis, I.A., Damste, J.S.S., 2002. Enhanced productivity led to increased organic carbon burial in the euxinic North Atlantic basin during the late Cenomanian oceanic anoxic event. Paleoceanography, 17: 1051.

Kuypers, M.M.M., Pancost, R.D., Sinninghe Damsté, J.S., 1999. A large and abrupt fall in atmospheric CO_2 concentration during Cretaceous times. Nature, 399: 342-345.

Larson, R.L., 1991. Geological consequences of super plumes. Geology, 19: 963-966.

Leckie, R.M., Bralower, T.J., Cashman, R., 2002. Oceanic anoxic events and plankton evolution: biotic response to tectonic forcing during the mid-Cretaceous. Paleoceanography, 17: 13.1-13.29.

Mahmudy Gharaie, M.H., Matsumoto, R., Kakuwa, Y., Milroy, G., 2004. Late Devonian facies variety in Iran: volcanism as a possible trigger of the environmental perturbation near the Frasnian-Famennian boundary. Geological Quarterly, 48(4): 323-332.

Meyers, P.A., 1997. Organic geochemical proxies of paleoceanographic, paleolimnologic, a paleoclimatic process. Organic Geochemistry. 27, 213-250.

Meyers, P.A., Bernasconi, S.M., Forster, A., 2006. Origins and accumulation of organic matter in Albian to Santonian black shale sequences on the Demerara Rise, South American margin. Organic Geochemistry, 37: 1816-1830.

Meyers, P.A., Bernasconi, S.M., Yum, J., 2009. 20 My of nitrogen fixation during deposition of mid-Cretaceous black shales on the Demerara Rise, equatorial Atlantic Ocean. Organic Geochemistry, 40: 158-166.

Mokhtari, M., Moussavi-Harami, R., Mahboubi, A., Khorasani, M., 1999. Application of three dimensional reflex seismic in sequence stratigraphy and petroleum exploration, Gonbadly and Khangiran gas field in northeastern Iran. 3rd Symposium of Iranian Geological Society, Shiraz University, 598-601.

Mort, H.P., Adatte, T., Keller, G., Bartels, D., Follmi, K.B., Steinmann, P., Berner, Z., Chellai, E.H., 2008. Carbon deposition and phosphorus accumulation during Oceanic Anoxic Event 2 in Tarfaya, Morocco. Cretaceous Research. 29: 1008-1023.

Moussavi-Harami, R., Brenner, R., 1990. Lower Cretaceous (Neocomian) fluvial deposits in eastern Kopet Dagh. Cretaceous Research, 11: 163-174.

Muttoni, G., Mattei, M., Balini, M., Zanchi, A., Gaetani, A., Berra, F., 2009. The drift history of Iran from the Ordovician to the Triassic. In: Geological Society of London, Special Publication: South Caspian to Central Iran Basin, pp. 7-29.

Nabavieh, S.M. 1998. Geological map of Kalate-Nader. Geological survey of Iran, scale 1:100000.

Ogg, J.G., Ogg, G., Gradstein, F.M., 2008. The Concise Geologic Time Scale, Cambridge University Press, 177 pp.

Okano, K., Sawada, K., Takashima, R., Nishi, H., Okada, H., 2007. Depositional environments revealed from biomarkers in sediments deposited during the mid-Cretaceous Oceanic Anoxic Events (OAEs) in the Vocontian Basin (SE France). Sapporo, 233-238.

Oliveira, A.; Vitorino, J.; Rodrigues, A.; Jouanneau, J.M.; Dias, J.M.A.; and Weber, A., 2002. Nepheloid layer dynamics of the northern Portuguese shelf. Progress in Oceanography, 195-213.

Parrish, J.T., 1998. Interpreting pre-Quaternary climate from the geologic record. Columbia Univ. Press.

Pearce, M.A., Jarvis, I., Tocher B.A., 2009. The Cenomanian-Turonian boundary event, OAE2 and palaeoenvironmental change in epicontinental seas: New insights from the dinocyst and geochemical records. Palaeogeography, Palaeoclimatology, Palaeoecology, 280, 207-234.

Pedersen, T.F., Calvert, S.E., 1990. Anoxia vs. productivity: What controls the formation of organic-carbon-rich sediments and sedimentary rocks? American Association of Petroleum Geologists Bulletin, 74: 454-466.

Pogge von Strandmann, P.A.E., Jenkyns, H.C., Woodfine, R.G., 2013. Lithium isotope evidence for enhanced weathering during Oceanic Anoxic Event 2. Nature Geoscience, 6: 668-672.

Pratt, L.M., Threlkeld, C .N., 1984. Stratigraphic significance of $^{12}C/^{13}C$ ratio in mid-Cretaceous rocks of the western interior, U. S. A. In: Stott, D.F., Glass, D.J. (Eds.), The Mesozoic of Middle North America. Canadian Society of Petroleum Geologists Memoir, pp. 305-312.

Premoli-Silva, I., Verga, D., 2004. Practical manual of Cretaceous planktic foraminifera. In: Verga, D., Rettori, R. (Eds.), International School on Planktic Foraminifera, University of Perugia and Milan.

Ramkumar, M., 2015, Toward standardization of terminologies and recognition of chemostratigraphy as a formal stratigraphic method, In: Ramkumar, M. (Ed.), Chemostratigraphy, concepts, techniques and applications. Elsevier, pp.

1-21

Robert, A.M.M., Letouzey, J., Kavoosi, M.A., Sherkati, S., Müller, C., Verges, J., Aghababaei, A. 2014: Structural evolution of the Kopet Dagh fold-and-thrust belt (NE Iran) and interactions with the South Caspian Sea Basin and Amu Darya Basin. Marine and Petroleum Geology, 57: 68 -87.

Robert, C., Kennett, J.P., 1997. Antractic continental weathering changes during Eocene-Oligocene cryosphere expansion: clay mineral and oxygen isotope evidence. Geology, 25(7): 587-590.

Schlanger, S.O., Jenkyns H.C., 1976. Cretaceous oceanic anoxic events: Causes and consequences. Geologie en Mijnbouw, 55: 179-184.

Schnyder, J.; Gorin, G.; Soussi, M.; Baudin, F.; Deconinck, J.F., 2005. Enregistrement de la variation climatique au passage Jurassique/Cretace sur la marge sud de la Tethys: mineralogy des argiles et palynofacies de la coupe du Jebel Meloussi (Tunisie Centrale, Formation Sidi Kralif). Bulletin de la Societe Geologique de France, 176 (2): 171-182.

Scholle, P.A., Arthur, M.A., 1980. Carbon isotope fluctuations in Cretaceous pelagic limestones: potential stratigraphic and petroleum exploration tool. American Association of Petroleum Geologists Bulletin, 64: 67-87.

Seton, M., Gaina, C., Muller, R.D., Heine C., 2009. Mid-Cretaceous seafloor spreading pulse: Fact or fiction?. Geology, 37: 687-690.

Singer, A., 1984. The paleoclimatic interpretation of clay minerals in sediments: a review. Earth Science Reviewer, 21(4): 251-293.

Sinninghe Damsté, J.S., Kuypers, M.M.M., Pancost, R.D., Schouten, S., 2008. The carbon isotopic response of algae, (cyano) bacteria, archaea and higher plants to the late Cenomanian perturbation of the global carbon cycle: Insights from bio markers in black shales from the Cape Verde Basin (DSDP Site 367). Organic Geochemistary, 39:1703-1718.

Snow, L.J., Duncan, R.A., 2001. Hydrothermal links between ocean plateau formation and global anoxia, Eos Trans. AGU, 82 (47). Fall Meeting Supplement, abstract OS41A-0437.

Takashima, R., Nishi, H., Hayashi, K., Okada, H., Kawahata, H., Yamanaka, T., Fernando, A.G., Mampuku, M., 2009. Litho, bio and chemostratigraphy across the Cenomanian/Turonian boundary (OAE 2) in the Vocontian Basin of southeastern France. Palaeogeography, Palaeoclimatology, Palaeoecology, 273: 61-74.

Tsikos, H., Jenkyns, H.C., Walsworth-Bell, B., 2004. Carbon-isotope stratigraphy recorded by the Cenomanian-Turonian Oceanic Anoxic Event: Correlation and implications based on three key localities. Journal of Geological Society, 161: 711-719.

Turgeon, S., Brumsack, H.J., 2006. Anoxic vs dysoxic events reflected in sediment geochemistry during the Cenomanian – Turonian Boundary Event (Cretaceous) in the Umbria– Marche Basin of central Italy. Chemical Geology, 234: 321-339.

van Bentum, E.C.; Reichart, G.J., Forster, A., Sinninghe Damst´, J.S., 2012. Latitudinal differences in the amplitude of the OAE-2 carbon isotopic excursion: pCO_2 and paleo productivity. Biogeosciences, 9: 717-731.

Voigt, S., Gale, A.S., Vioigt, T., 2006. Sea level change, carbon cycling and palaeoclimate during the Late Cenomanian of northwest Europe; an integrated palaeoenvironmental analysis. Cretaceous Research, 27: 836-858.

Weissert, H., Joachimski, M., Sarnthein, M., 2008. Chemostratigraphy. Newsletters on Stratigraphy, 42(3): 145-179.

Wortmann, U.G., Hesse, R. and Zacher, W., 1999. Major-element analysis of cyclic black shales: Paleoceanographic implications for the Early Cretaceous deep western Tethys. Paleoceanography, 14: 525–542.